scientific reports

Check for updates

OPEN

NopP2 effector of *Bradyrhizobium elkanii* USDA61 is a determinant of nodulation in *Vigna radiata* cultivars

Pongdet Piromyou[1,7], Natcha Pruksametanan[2,7], Hien P. Nguyen[3,6,7], Pongpan Songwattana[1], Jenjira Wongdee[1], Phongkeat Nareephot[2], Teerana Greetatorn[1], Kamonluck Teamtisong[4], Panlada Tittabutr[2], Nantakorn Boonkerd[2], Shusei Sato[5], Pakpoom Boonchuen[2]✉, Shin Okazaki[3]✉ & Neung Teaumroong[2]✉

The symbiotic relationship between legumes and rhizobia is known to be influenced by specific rhizobial type III effectors (T3Es) in certain cases. In this study, we present evidence that the symbiosis between *Vigna radiata* and *Bradyrhizobium elkanii* USDA61 is controlled by a T3E called NopP2, and this interaction is highly dependent on the genetic makeup of the host plant. NopP2 plays a crucial role in promoting nodulation in various *V. radiata* varieties. Additionally, NopP2 is essential for early infection and the formation of nodules in compatible plants. Through evolutionary analysis, we discovered that bradyrhizobial NopPs can be categorized into two distinct clusters: NopP1 and NopP2. Furthermore, both types of bradyrhizobial NopPs were conserved within their respective groups. Our findings suggest that NopP2 serves as a mechanism for optimizing the symbiotic relationship between *V. radiata* and *B. elkanii* USDA61 by interacting with the pathogenesis related-10 (PR10) protein and reducing effector-triggered immunity (ETI) responses.

Keywords T3SS, Effector protein NopP, *Bradyrhizobium elkanii* USDA61, *Vigna radiata*, Pathogenesis related-10 (PR10) protein

Symbiosis between legumes and rhizobia in root nodules facilitates the utilization of atmospheric dinitrogen through nitrogen fixation reactions. Rhizobia, which are naturally occurring soil bacteria, encompass a vast array of species that form symbiotic partnerships with various legume plants. In this mutualistic interaction, legume plants produce flavonoids, which serve as crucial signaling molecules recognized by specific rhizobia, thereby triggering the activation of *nod* genes[1]. However, numerous rhizobia have evolved diverse strategies to optimize their symbiotic interaction with host plants. Among these strategies, a multitude of rhizobial type III secretion systems (T3SSs) are involved in the nodulation process by delivering type three effectors (T3Es) directly into the cytosol of eukaryotic host cells, which are referred to as nodulation outer proteins (Nops)[2]. Plant flavonoids activate the transcriptional regulator NodD, which then induces the expression of the T3SS transcription regulator (*ttsI*)[3]. Several T3Es can suppress plant defense reactions, thereby promoting nodulation symbiosis[4–7], whereas some T3Es also exhibit incompatibility with nodulation[8,9].

For *Vigna mungo*, several T3Es (NopP2, Bel2-5, and InnB) also impact the mutualistic effectiveness depending on the host cultivar[10]. Although many rhizobial T3Es have been characterized[11,12], the specific relationships between *V. radiata* and T3Es, which are dependent on the genotypic compatibility or incompatibility of the legumes, have remained largely unexplored until now.

[1]Institute of Research and Development, Suranaree University of Technology, Nakhon Ratchasima 30000, Thailand. [2]School of Biotechnology, Institute of Agricultural Technology, Suranaree University of Technology, Nakhon Ratchasima 30000, Thailand. [3]Institute of Global Innovation Research (IGIR), Tokyo University of Agriculture and Technology (TUAT), Fuchu, Tokyo 183-8538, Japan. [4]The Center for Scientific and Technological Equipment, Suranaree University of Technology, Nakhon Ratchasima 30000, Thailand. [5]Graduate School of Life Sciences, Tohoku University, Sendai 980-8577, Japan. [6]School of Medicine and Pharmacy, Duy Tan University, Danang City 550000, Vietnam. [7]These authors equally contributed as co-first authors: Pongdet Piromyou, Natcha Pruksametanan and Hien P. Nguyen. ✉email: pakpoom.b@sut.ac.th; sokazaki@cc.tuat.ac.jp; neung@sut.ac.th

Previous research has revealed the involvement of the *Bradyrhizobium elkanii* USDA61 T3SS in restricting nodulation in *V. radiata* cv. KPS1[13]. Mutation of the T3SS has been shown to induce distinct symbiotic phenotypes, but the USDA61 wild-type strain exhibited a near-total abolition of nodulation. Interestingly, the InnB effector USDA61 is responsible for host-specific nodulation restriction in *V. radiata* KPS1[14]; thus, the effector *innB*-deficient mutant (BEinnB) was compared with the T3SS-deficient strain (BErhcJ). Compared with BErhcJ inoculation, BEinnB drastically increased symbiosis with *V. radiata* KPS1, suggesting that InnB plays important roles in controlling host-species-specific symbiotic interactions. However, a comparison of nodulation efficiency between BErhcJ and BEinnB implied that USDA61 employs additional T3Es to facilitate symbiosis with *V. radiata* KPS1[14]. Despite these discoveries, the precise symbiotic implications of the *B. elkanii* T3SS in *V. radiata* cultivars have remained uncertain.

V. radiata is an important crop legume in Thailand that is consumed and used in various types of food. However, in organic farming systems, the application of rhizobial inoculants has not been as successful as expected. This may be due to the effectiveness of the rhizobial inoculants and the competition from local strains, which are less effective than commercial strains. This could be attributed to the T3SS system, which can have either positive or negative effects on nodulation in legumes.

Hence, the present study aims to shed further light on the roles of the bradyrhizobial T3SS as a determining factor for symbiosis with *V. radiata* cultivars. According to previous reports, NopP is a major positive determinant of nodulation in some tropical legumes, such as *Flemingia congesta* and *Tephrosia vogelii*[6], but it displays negative incapability of *V. radiata* symbiosis[8]. NopP is found in various strains of rhizobium genera; however, its role in promoting mutualistic symbiosis in *V. radiata* has not yet been reported. Therefore, this study focused on investigating the role of NopP in *V. radiata* symbiosis. Our findings provide compelling evidence that T3SS-triggered symbiosis relies on a combination of T3Es, with NopP2 emerging as a crucial player essential for early infection establishment and nodule organogenesis.

Results

Phylogenetic analyses and gene localization of bradyrhizobial NopP1 and NopP2

NopP is an effector secreted by the T3SS of various rhizobial species. Its function is not clearly understood, and it has no homology with any avirulence (Avr) effectors in pathogens[9]. To gain insight into the evolutionary history of bradyrhizobial NopPs, we conducted a phylogenetic analysis to examine the relationships among NopP homologs. The rhizobium genera included in this study were *Sinorhizobium*, *Mesorhizobium*, *Rhizobium* and *Ensifer*. Additionally, the bradyrhizobium species *Bradyrhizobium elkanii*, *B. diazoefficiens* and *B. japonicum* were also included. Our findings revealed that bradyrhizobial NopPs can be categorized into two distinct clusters: NopP1 and NopP2. Furthermore, both types of bradyrhizobial NopPs were conserved within their respective groups (Fig. 1). Among the various NopP1s, a close phylogenetic relationship between *B. elkanii* NopP1s and homologs in *Microvirga* sp. KLBC81, *Microvirga* sp. HBU67558 and *Mi. calopogonii* was observed (Fig. 1), whereas the *Ensifer* clade was slightly separated from the *B. elkanii* clade. In contrast, NopP1 homologs of the *Mesorhizobium* group and *R. leguminosarum* bv. *phaseoli* were separated from another *B. elkanii* NopP1.

When the evolution of NopP2 was considered, it was distinctly separated from that of NopP1. USDA61 NopP2 was grouped with *B. elkanii*, with the exception of *Bradyrhizobium* sp. BRP56, which is also included in this group. Interestingly, both the NopP2 groups of *B. japonicum* and *B. diazoefficiens* were evolutionarily related. Among the bradyrhizobium species analyzed, the majority were found to possess at least one copy of NopP. Notably, *B. japonicum* and *B. diazoefficiens* commonly had a single copy (NopP2), whereas NopP1 was absent in almost all *B. japonicum* and *B. diazoefficiens*, except for *B. diazoefficiens* 657 (Fig. 1). In the cases of *Ensifer* and *Mesorhizobium*, only NopP1 was detected, whereas NopP2 was not detected. Interestingly, *B. elkanii* contained both NopP1 and NopP2, with the evolution of NopP clearly distinct from that of other *Rhizobium* species. When the arrangement of the genes *nopP1* and *nopP2* in the genome of USDA61 was considered, *nopP2* was found to be located within the symbiotic island near the *nif* cluster (Figs. S1A and S1C). In contrast, *nopP1* was located further from the symbiotic island and was located near transposases (Figs. S1A and S1B). Moreover, the role of NopP in *B. elkanii* in promoting mutualistic interactions with legume plants, particularly *V. radiata*, has not been elucidated before. Therefore, to determine the role of NopP in promoting symbiosis in *V. radiata* root nodules, we constructed and tested mutants of these genes in subsequent experiments.

Functional analysis of *B. elkanii* NopP2 in determining the nodulation of *V. radiata* KPS1

To understand the positive role of other T3Es, the T3E mutants from a previous work[10] were preliminarily investigated using single mutations of *nopL* (BEnopL), *nopP1* (BEnopP1), *nopP2* (BEnopP2), and *bel2-5* (BE5208) and double mutations of both *innB*/*nopP*$_2$ (BEinnBnopP2) and *innB*/*bel2-5* (BEinnB5208). The nodulation efficiency of T3E-deficient strains (BEnopL, BEnopP1, BEnopP2 and BE5208) was not significantly different from that of BErhcJ-inoculated strains, whereas BEinnB strongly promoted nodulation in *V. radiata* KPS1 (Fig. S2). Moreover, the BEinnBnopP2 double mutation strain exhibited significantly lower symbiotic efficiency than BEinnB inoculation did (Fig. 2 and 3), but its BEinnBnopP2 deletion mutant induced *V. radiata* KPS1 phenotypes similar to those of BErhcJ inoculation. These findings suggest that USDA61-nopP2 plays a crucial beneficial role in *V. radiata* KPS1 symbiosis (Fig. 2). To confirm the role of NopP2, *nopP2* complementation into the BEinnBnopP2 background (BEinnBnopP2::nopP2) was employed. The results revealed that BEinnBnopP2::nopP2 enhanced KPS1 nodulation to the same degree as BEinnB did (Fig. 2). However, BEinnB5208 did not significantly differ from BEinnB in terms of the *V. radiata* KPS1 phenotype (Fig. S2), suggesting that *bel2-5* does not contribute symbiotic properties to *V. radiata* KPS1 symbiosis.

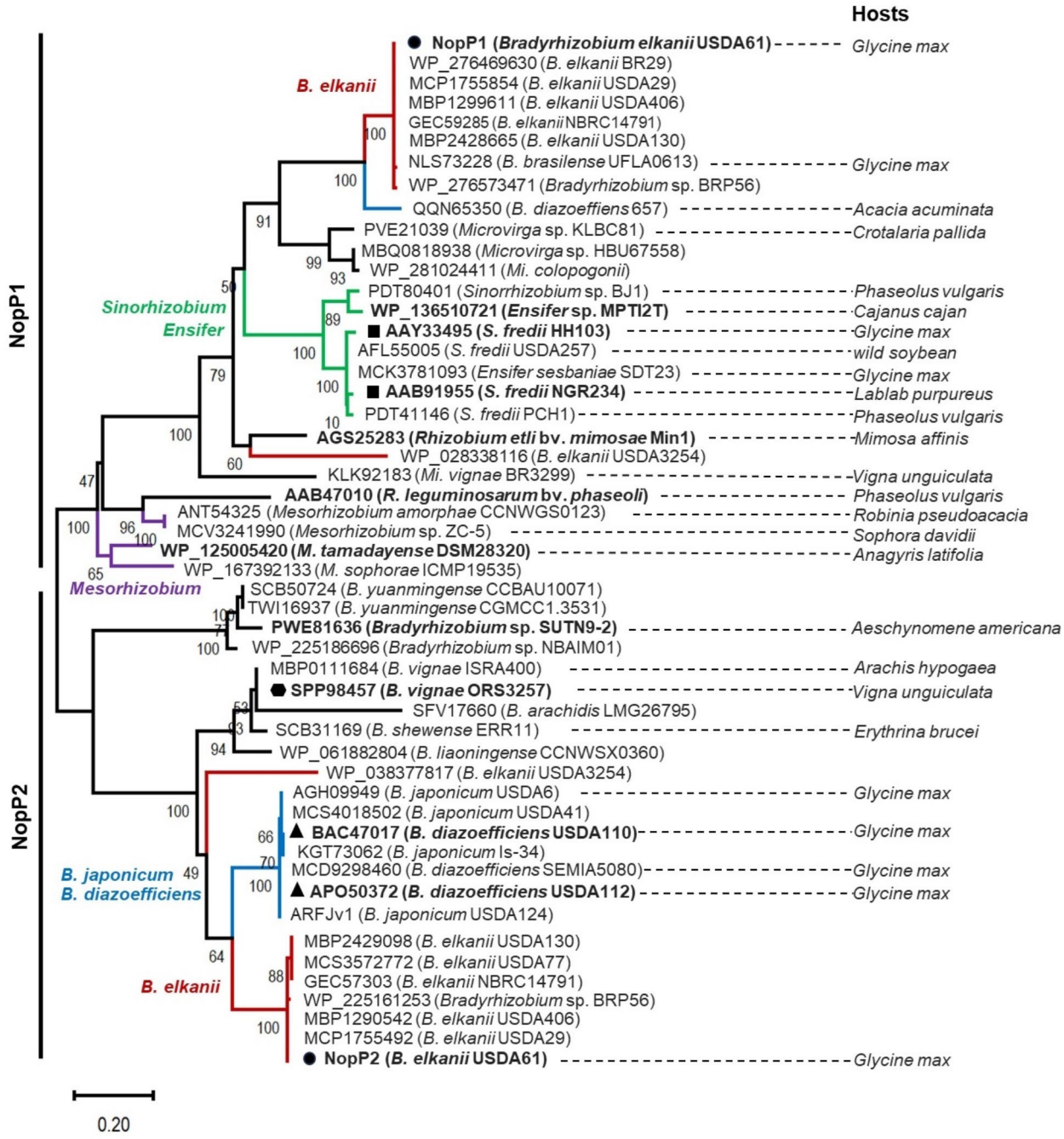

Fig. 1. Phylogenetic analysis of *Bradyrhizobium elkanii* USDA61 NopPs and their homologs among rhizobia was constructed using the Maximum Likelihood method. The analysis used the Jones-Taylor-Thornton (JTT) and Gamma Distributed (G) models, with 1,000 bootstrap replications. NopPs of *B. elkanii* (red), *B. japonicum*/*B. diazoefficiens* (blue), *Sinorhizobium*/*Ensifer* (green), and *Mesorhizobium*/*Rhizobium* (purple) groups are highlighted in line. The main hosts or hosts from which the rhizobial strains were first isolated are shown. The symbols (●), (▪), (▲) and (⬢) indicate the nodulation of rhizobial strains previously tested with *V. radiata* (*B. elkanii*, *Sinorhizobium* sp., *B. vignae* and *B. diazoefficiens*, respectively).

Nodulation of *V. radiata* induced by USDA61-nopP2

To further investigate the role of NopP2 in promoting symbiosis, we examined nodulation-related organogenesis in *V. radiata* KPS1 roots inoculated with BEinnB or BEinnBnopP2 at 11 and 15 days post inoculation (dpi) (Fig. 3). At the early stage of nodulation (11 dpi), BEinnBnopP2 inoculation caused a significant reduction in nodule primordia formation in *V. radiata* KPS1 roots compared with BEinnB, which had already formed young nodules (Fig. 3A and C). At 15 dpi, the number of young nodules established by BEinnBnopP2 inoculation was still drastically lower than that formed by BEinnB inoculation (Fig. 3B and D). Although each single nodule

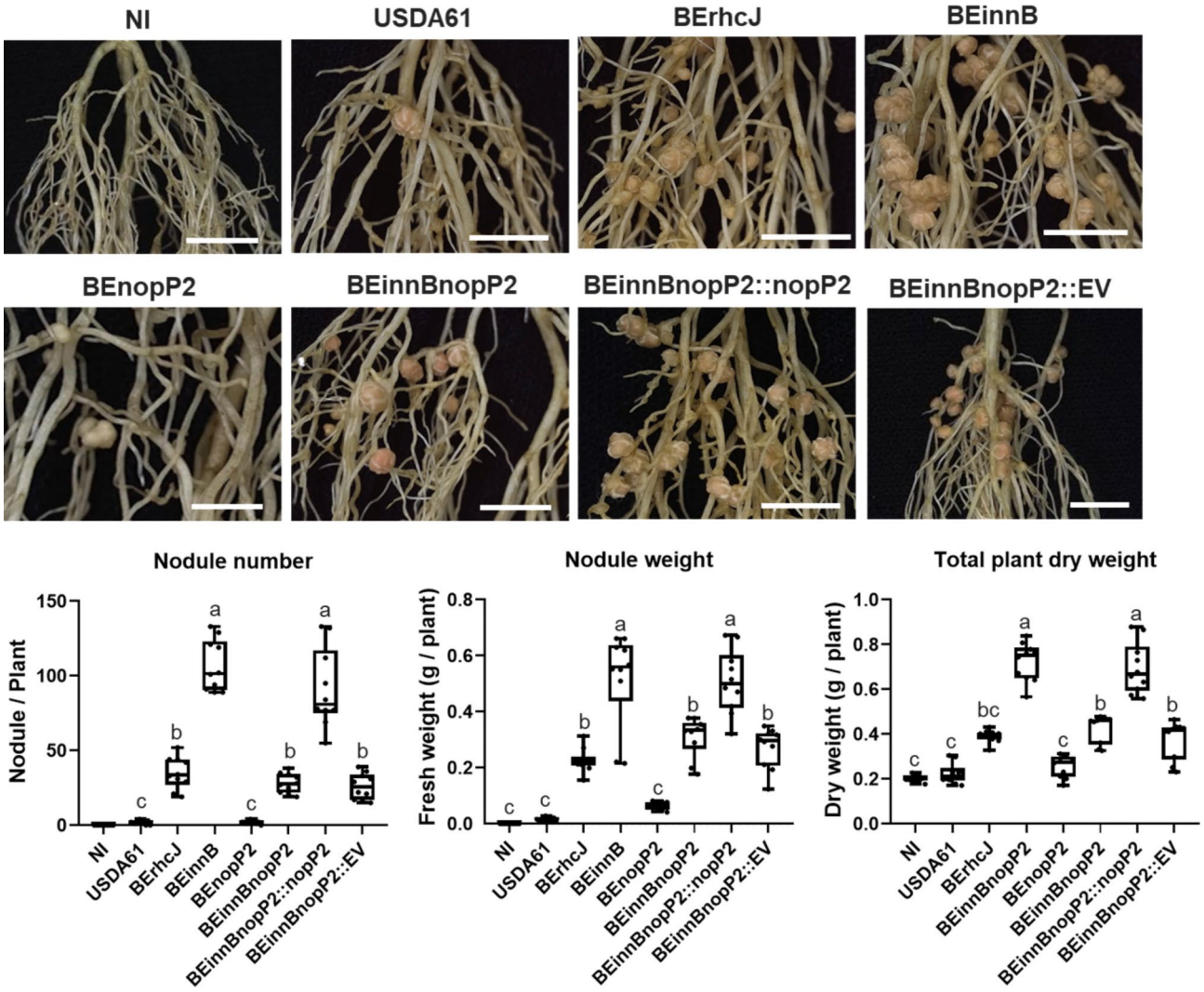

Fig. 2. Symbiotic properties of *Vigna radiata* KPS1 inoculated with *B. elkanii* USDA61 and its mutant derivatives. Cytological analysis of the nodules induced by strains USDA61, BErhcJ, BEinnB, BEnopP2, BEinnBnopP2, BEinnBnopP2::nopP2 and BEinnBnopP2::EV (empty vector) observed via stereomicroscopy (roots of KPS1; scale bars: 1 cm), nodule number, fresh nodule weight and total plant dry weight of KPS1 plants. The data shown are the means of 10 plant inoculation assays at 30 dpi. The data shown are box and whisker plots. Means followed by different letters are significantly different at the 5% level, "**" $P < 0.05$ according to Student's *t* test.

morphology did not seem to differ between BEinnB and BEinnBnopP2, more bacteroid cell death was observed in BEinnBnopP2 than in BEinnB (Fig. 3B).

To evaluate the impact of USDA61-NopP2 on various genetic interactions in *V. radiata*, we inoculated various *V. radiata* cultivars with the BEinnB and BEinnBnopP2 bradyrhizobial strains (Fig. 4 and Table S1). Compared to BEinnB, the growth of *V. radiata* CN72, KPS2, and SUT4 was significantly lower with BEinnBnopP2 inoculation. BEinnBnopP2 resulted in the formation of fewer nodules (approximately 4–15 nodules per plant, depending on the cultivar) than did BEinnB, which produced significantly more symbiotic nodules (approximately 100 nodules per plant) on the CN72 and KPS2 cultivars. However, the nodule morphology in each cultivar was similar when BEinnB and BEinnBnopP2 were inoculated. The bacteroid cells derived from BEinnB were still alive inside *V. radiata* nodules, whereas bacteroid cell deaths were more common in nodules from BEinnBnopP2-inoculated plants (Fig. 4). Among the 12 *V. radiata* cultivars tested, BEinnB promoted *V. radiata* symbiosis better than that of BEinnBnopP2. (Table S1).

Phylogenetic tree analysis revealed that USDA61-nopP2 clusters with *B. diazoefficiens* USDA122-nopP2, *B. diazoefficiens* USDA110-nopP2, and *B. vignae* ORS3257-nopP2. However, ORS3257-nopP2 clearly inhibits nodule formation in *V. radiata*[8], and USDA122-nopP2 also has a negative effect on nodule formation in KPS1[9]. In contrast, USDA110-nopP2 has positive effects on KPS1 nodulation[9], similar to USDA61-nopP2. To clarify the positive effects of NopP2 on KPS1 symbiosis, we tested the impact of USDA61-nopP2 compared with USDA110-nopP2 at 11 and 15 dpi (Fig. S3). The results revealed that the USDA110-nopP2-deficient (110nopP) strain had

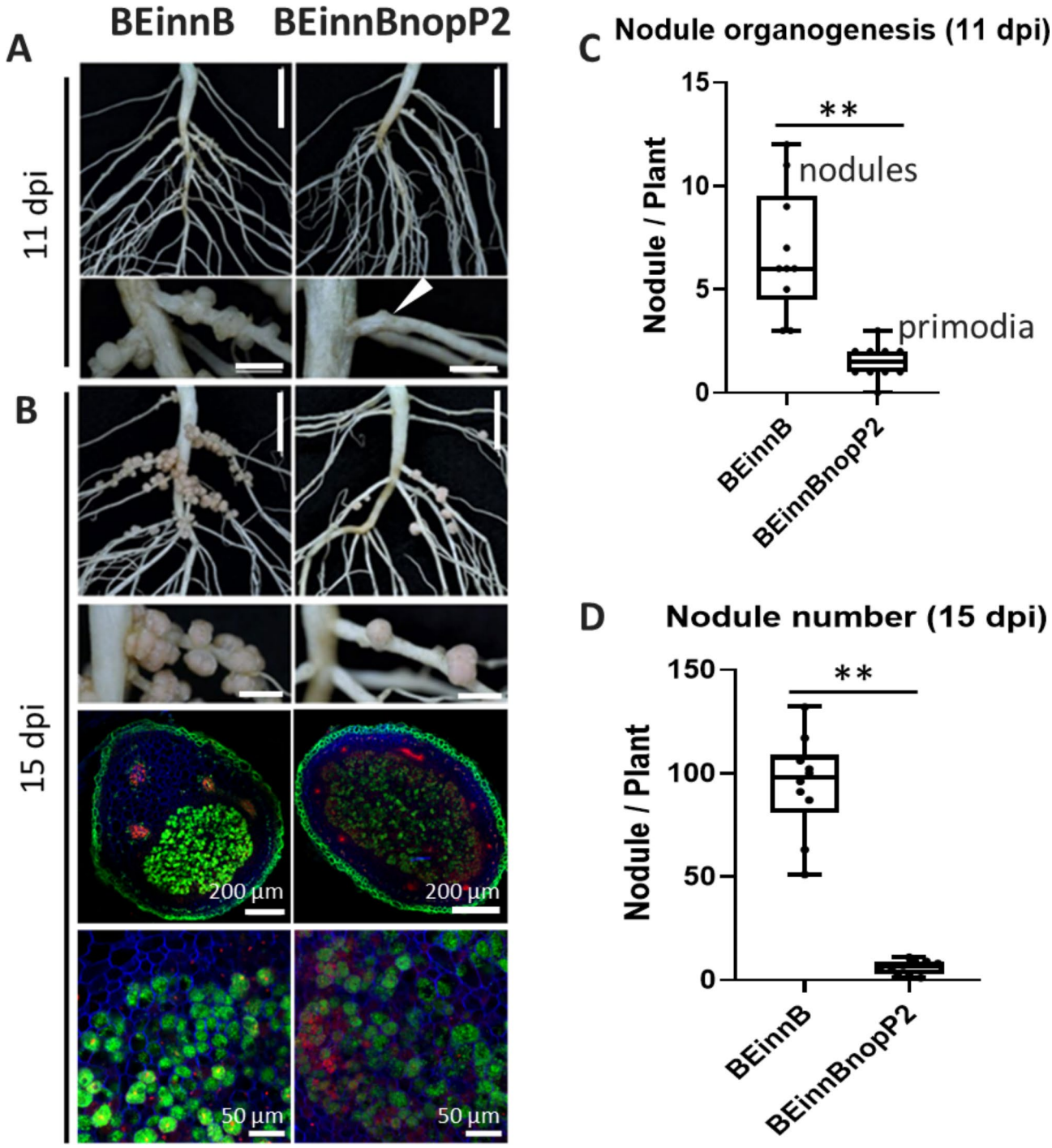

Fig. 3. Nodulation properties of *V. radiata* KPS1 inoculated with *B. elkanii* strains. The roots were imaged at 11 (**A**) and 15 (**B**) dpi. Cytological analysis of the nodules induced by strains BEinnB and BEinnBnopP2 observed by confocal microscopy after staining with SYTO9 (green: live bacteria), calcofluor (blue: plant cell wall), and propidium iodide (red; infected plant nuclei and dead bacteria or bacteria with compromised membranes). The white arrowhead in Figure-A shows the primordia. (**C**) Nodule organogenesis of root tissue (11 dpi) and (**D**) numbers of young nodules per plant observed at 15 dpi. The data shown are box and whisker plots of 10 plants. Scale bars: 1 cm, nodule primordia and young nodules; "**" $P < 0.01$ according to Student's *t* test.

a similar effect on USDA110 wild-type (USDA110) inoculation (producing approximately 40–50 nodules per plant). In contrast, BEinnBnopP2 resulted in the least amount of nodule formation (approximately 3–5 nodules per plant), but the BEinnB strain led to the greatest amount of nodule formation (approximately 100 nodules per plant). These findings suggest that USDA61-nopP2 clearly has a positive effect on KPS1 nodulation compared with USDA110-nopP2.

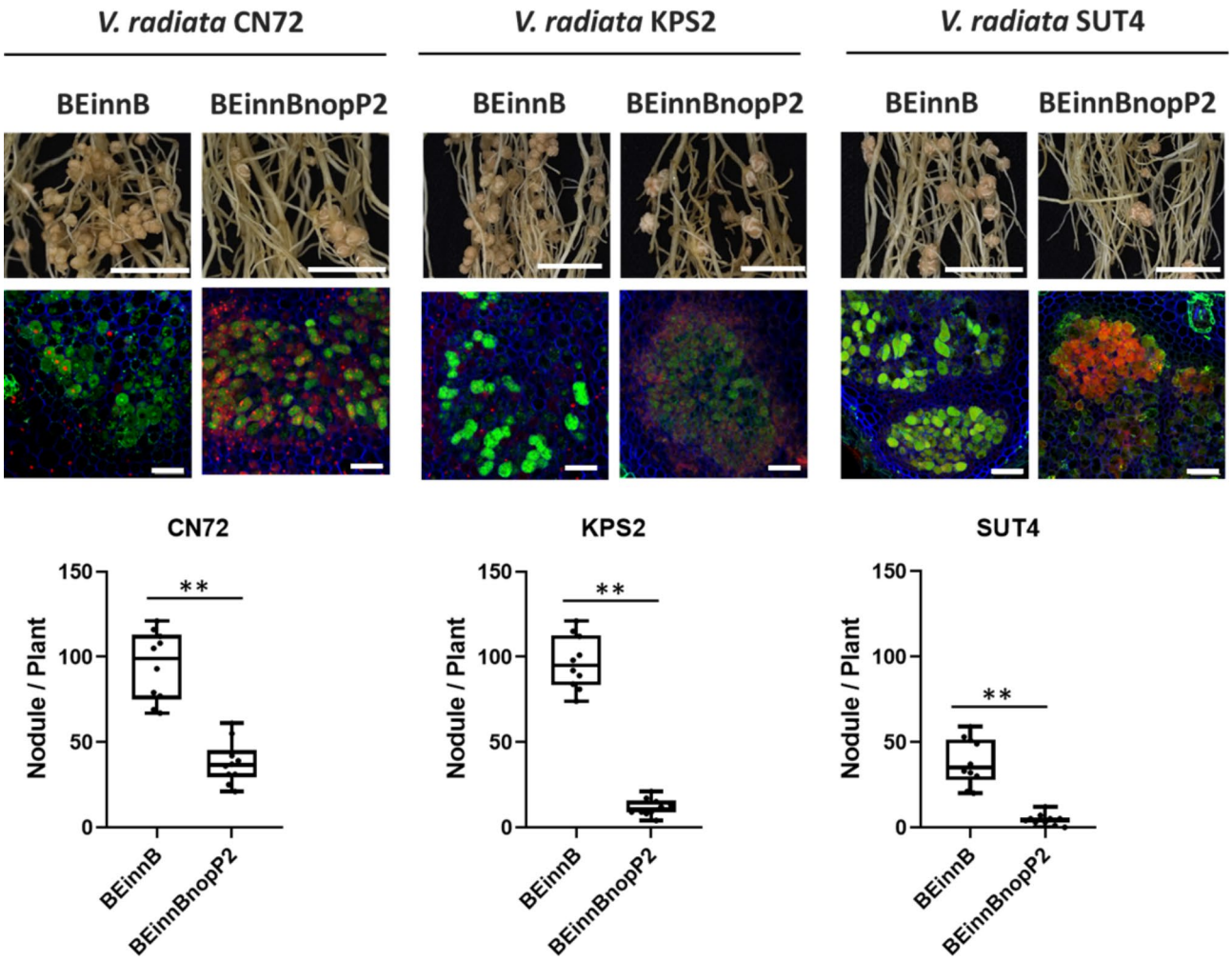

Fig. 4. Nodulation properties of *V. radiata* CN72, KPS2 and SUT4 inoculated with *B. elkanii* strains. Roots were imaged at 30 dpi, and cytological analysis of the nodules induced by strains BEinnB and BEinnBnopP2 was performed via confocal microscopy after staining with SYTO9, calcofluor, and propidium iodide. Nodule numbers of CN72, KPS2 and SUT4 observed at 30 dpi. The data shown are box and whisker plots of 10 plants. Scale bars: 1 cm, nodule primordia and young nodules; "**" $P < 0.01$ according to Student's *t* test.

V. radiata transcriptomic analysis in response to the USDA61-T3Es (innB and nopP2) effector

The aim of the transcriptomic analysis was to elucidate the mechanisms involved in the early stage of nodulation (4 dpi) influenced by NopP2 effectors in *V. radiata* KPS1. A total of nine libraries generated approximately 40–50 million total reads. Among them, more than 97% of the reads from Q20 were clean (Table S5). A total of 33 differentially expressed genes (DEGs) were discerned on the basis of filtering data at an FDR < 0.05 and $\log_2$ (fold change) > 1, which were compared between genes in the BEinnB- and BEinnBnopP2-inoculated groups. The total number of upregulated genes and downregulated genes was 2 and 31, respectively (Fig. 5A). Differentially expressed genes (DEGs) were analyzed using Gene Ontology (GO) functional enrichment analysis (Fig. 5B). The number of DEGs significantly changed (P value ≤ 0.05) in each bradyrhizobial inoculation were analyzed. To better understand the impact of NopP2 effectors on the response of KPS1, a comparison of the genes differentially expressed between the BEinnB and BEinnBnopP2 treatments was performed (Fig. 5C). The upregulated DEGs were associated with protein sieve element occlusion B and protein FEZ, both of which are related to cell division. Interestingly, the downregulated genes were involved in root infection and nodule formation, including early nodulin 55 (ENOD55), early nodulin 75 (ENOD75), nodulin 21, nodulin 26, germin-like protein subfamily 1 (GLP subfamily 1), metalloendoproteinase 1 (MMPL1), gibberellin 20 oxidase (GA20ox), CASP-like protein N24 (CASP-N24), formin protein 4, flavin-containing monooxygenase 1 (FMO1), fotillin-like gene 4 (FLOT4) and L-tryptophan-pyruvate aminotransferase 1 (Fig. 5C). We also observed similar levels of genes involved in the defense pathway, such as WRKY transcription factor 12, WAT1-related protein, aspartic protease At2g35615, and allene oxide synthase 2, which are known to play roles in plant immune responses against pathogenic invasion. These results suggest that BEinnBnopP2 has fewer symbiotic interactions with *V. radiata* KPS1 than does BEinnB by impeding root infection and nodule organogenesis. To confirm the

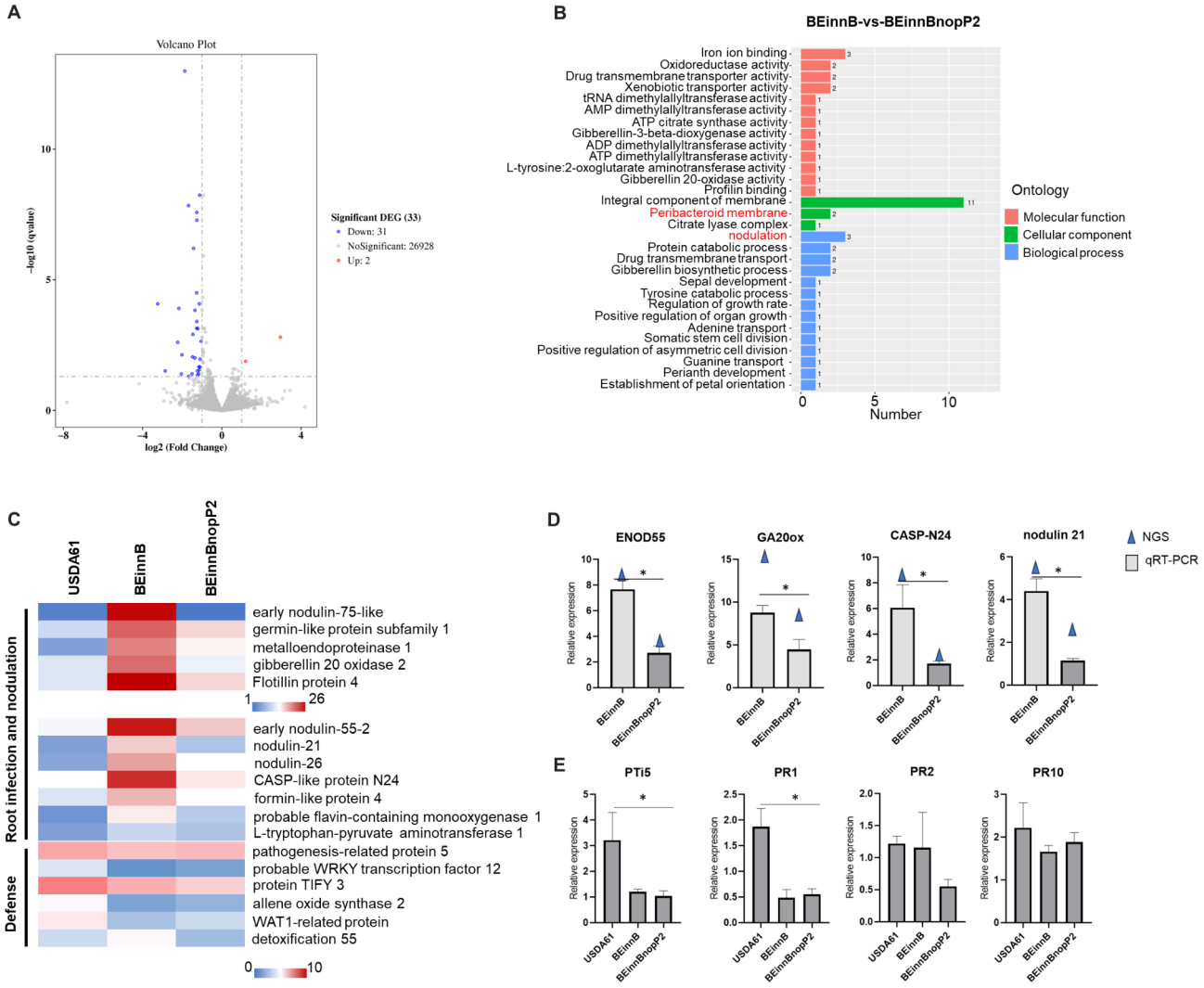

Fig. 5. Differentially expressed genes (DEGs) in *V. radiata* KPS1 inoculated with USDA61, BEinnB or BEinnBnopP2. (**A**) The total number of upregulated genes and downregulated genes was 2 and 31, respectively (**B**) GO functional analysis of DEGs in the BEinnB vs. BEinnBnopP2 treatment groups. (**C**) The expression patterns of DEGs of USDA61, BEinnB and BEinnBnopP2 are focused on and displayed as the $\log_2$-fold change ($Padj < 0.05$) of the DEGs. The color scale bars indicate normalized expression levels of DEGs from USDA61, BEinnB, and BEinnBnopP2. The heatmap was constructed via Microsoft Excel 365. (**D**) qRT-PCR verification from RNA-seq analysis data for *V. radiata* KPS1 between BEinnB and BEinnBnopP2 inoculation at and 4 dpi. (**E**) qRT-PCR of pathogenetic-related data at 1 dpi. Significance is indicated by the mean ± standard deviation ($n = 3$), "*", $P < 0.05$ according to Student's *t* test.

transcriptome data, the expression levels of 4 plant symbiosis-related genes were verified by qRT-PCR analysis. qRT-PCR was performed for genes associated with GO terms such as early nodulin 55 (ENOD55), gibberellin 20 oxidase (GA20ox), CASP-like protein N24 (CASP-N24), and nodulin 21 in *V. radiata* KPS1. The expression of these genes significantly differed between the BEinnB and BEinnBnopP2 inoculation groups, the results of which were similar to those of the transcriptome analyses (Fig. 5D). These results revealed that genes related to infection and nodule organogenesis were more highly expressed in BEinnB than in BEinnBnopP2. This finding is consistent with a previous finding that BEinnBnopP2 delays primordia formation in the early stages of nodule organogenesis compared with BEinnB. The genes related to the nodulation process of *V. radiata* were highly expressed at 4 days of BEinnB infection. Therefore, to understand the process more clearly at the early stage, we investigated the expression of KPS1 genes related to the plant immune system at 1 dpi. These genes included the pathogenesis-related genes transcriptional activator (PTi5), pathogenesis-related protein 1 (PR1), PR2, and PR10 (Fig. 5E). The results revealed that the PTi5 and PR1 genes were highly expressed after USDA61 inoculation, whereas BEinnB and BEinnBnopP2 presented significantly lower expression of these genes than USDA61 did. Additionally, PR2 and PR10 gene expression did not significantly differ across all of the experiments. These results indicate that USDA61-InnB inhibits the nodulation of KPS1 roots by activating the plant immune system. However, the mechanism by which USDA61-NopP2 promotes mutualistic symbiosis remains unclear. Therefore,

we conducted experiments to test the interaction of USDA61-NopP2 with biomolecules in plant cells, as shown below.

USDA61-NopP2 and *V. radiata* KPS1 interacting proteins targeted

To gain more insight into the role of NopP2 in *B. elkanii* USDA61 in promoting symbiotic interactions with *V. radiata* KPS1, we determined the interactions between the USDA61-NopP2 effector and *V. radiata* KPS1 root proteins using an in vitro pull-down assay. The purified NopP2-GST was used as bait to capture total root proteins from *V. radiata* KPS1 after USDA61 inoculation (Fig. 6). The candidate plant-interacting proteins revealed two significantly intense bands in the rNopP2-GST versus root protein combination treatment (Fig. 6A), whereas these bands were not detected in the treatments with either rNopP2-GST or plant root protein alone. These candidate bands were selected for MS/MS analysis, which identified the top amino acid sequence matches in the database: band 1 was adenosylhomocysteinase, and band 2 was pathogenesis-related protein 10 (Fig. 6B).

To confirm the interaction between the NopP2 effector and plant proteins, an in vitro pull-down assay was performed using individually purified proteins. Both candidate plant proteins were tagged with 6×-His, and the full-length sequence of each plant protein was also overexpressed in the pET system, while NopP2 was tagged with GST. The results demonstrated that recombinant adenosylhomocysteinase (rAD) protein was not detected in the rNopP2-GST versus rAD combination treatment (Fig. 7A), indicating that there was no interaction between adenosylhomocysteinase and USDA61-NopP2. Conversely, recombinant rNopP2-GST was found interaction in the rNopP2-GST versus rPR10 combination treatment (with a protein molecular weight of approximately 17 kDa) (Fig. 7B). Therefore, the interaction between rNopP2-GST and rPR10 was further confirmed via ELISA (Fig. 7C). Purified rPR10-His was immobilized, and different concentrations of rNopP2-GST (0–5 μM) were added to the rPR10-coated plate. The absorbance of anti-GST increased with increasing concentration of rNopP2-GST added, whereas the absorbance of anti-GST did not change with increasing rGST. These results indicate that PR10 can directly bind to USDA61-NopP2.

Discussions

Efficient nodulation of *V. radiata* by *Bradyrhizobium* species, including *B. elkanii* USDA61, *B. diazoefficiens* USDA110, *B. diazoefficiens* USDA122 and *B. vignae* ORS3257, has been reported. Previous findings demonstrated that the NopP effectors from *B. diazoefficiens* USDA110 slightly promoted nodulation in *V. radiata* KPS1[9], whereas NopP from *B. diazoefficiens* USDA122 hindered symbiotic nodulation[9]. Additionally, the NopP2 protein from *B. vignae* ORS3257 is also responsible for incompatibility with *V. radiata* symbionts[8], highlighting the critical role of NopPs in regulating *V. radiata*-specific symbiotic interactions; thus, NopP2 is not always successful or efficient for *V. radiata* symbiosis. Therefore, to further understand the evolutionary history

A

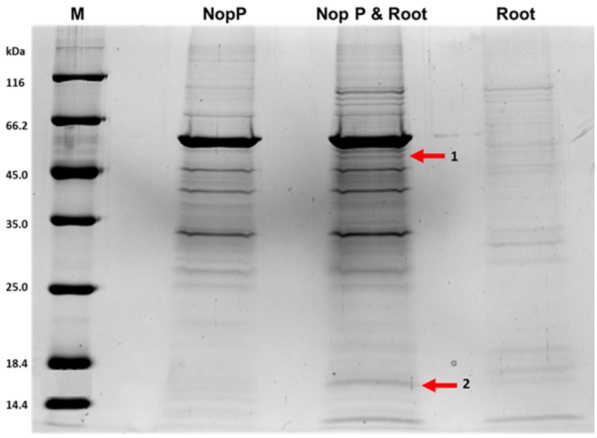

B

Analysis Method	Protein band	Protein name	Sequence Coverage (%)	pI	Molecular weight		NCBI accession no	Score
					Observed	Theory		
SDS-MS/MS	Band 1	Adenosylhomocysteinase	27	5.72	55	53.67	A0A1S3TJU8	139
	Band 2	Pathogenesis-related protein 10	47	4.60	16	16.18	Q2VU97	131

Fig. 6. SDS-PAGE of the pull-down assay. (**A**) SDS-PAGE; lane NopP, elution fraction from the pull-down assay of rNopP2-GST; lane NopP & Root, elution fraction from the pull-down assay of rNopP2-GST and root protein; lane Root, elution fraction from the pull-down assay of root protein. The numbers on the left of the panels indicate the positions of the molecular mass markers (Lane M) in kDa. (**B**) Candidate proteins derived from the pull-down assay, which were analyzed via SDS-MS/MS.

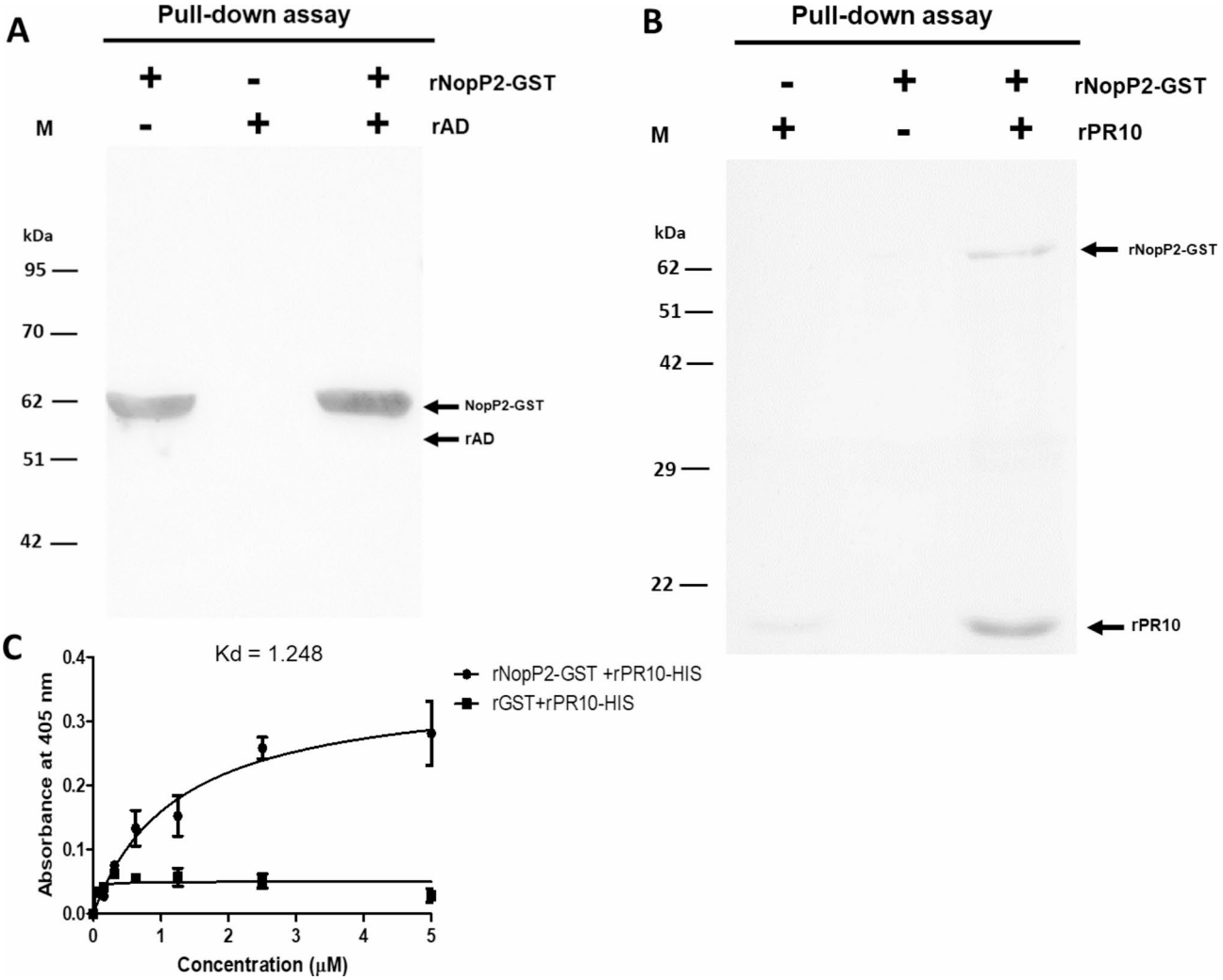

Fig. 7. Western blot analysis of the in vitro pull-down assay. Lane M, protein molecular weight marker. Glutathione Sepharose was used to perform the pull-down assay. Fifteen microliters were loaded into each lane. In vitro pull-down assay of protein–protein interactions between the recombinant root proteins and rNopP2. The binding of rAD (**A**) or rPR10 (**B**) to rNopP2 was assayed. The protein–protein complexes were separated via 12% SDS–PAGE and analyzed via Western blotting with an anti-His antibody and an anti-GST antibody. (**C**) Binding affinity between rNopP2-GST and rPR10-HIS determined by ELISA. The purified rPR10-HIS was immobilized. Recombinant NopP2-GST or rGST (0–5 μM) was added to a purified recombinant pathogen-related protein 10-coated plate, followed by probing with mouse anti-GST as the specific primary antibody and a goat anti-mouse-conjugated HRP secondary antibody. Finally, after the addition of the 2,2'-azinobis [3-ethylbenzothiazoline-6-sulfonic acid]-diammonium salt (ABTS) substrate, the absorbance at 405 nm (A 405) was measured. The solid lines represent the fitted curves.

of NopPs, phylogenetic analysis using NopP amino acid sequence was performed among rhizobial genera (Fig. 1). NopP rhizobia were predominantly found in *Bradyrhizobium*, although several were also identified in *Mesorhizobium*, *Microvirga*, and *Sinorhizobium/Ensifer*. Notably, many of these rhizobia can efficiently nodulate or are the main symbionts of *Vigna* spp. (Fig. 1). Unlike other rhizobium-specific T3Es, the NopP2 homolog was not identified in *Mesorhizobium* sp., *Rhizobium* sp., or *Sinorhizobium* sp./*Ensifer* sp. Surprisingly, *B. japonicum* and *B. diazoefficiens* were found to have only NopP2, except for *B. diazoefficiens* 657. The *B. elkanii*-NopP2 group was phylogenetically related to the NopPs of the *B. japonicum*/*B. diazoefficiens* clade, which are primarily soybean (*Glycine max*) symbionts (Fig. 1). The phylogenetic relationship of NopP2 suggests that the *B. elkanii* clade and the *B. japonicum*/*B. diazoefficiens* clade might initially recruit the *nopP2* gene in a similar manner; subsequently, the evolution of *nopP2* began to diverge. This finding implied that *Bradyrhizobium* species continuously experience changes in *nopP2*, with even minor genetic changes significantly impacting their ability to form nodules in soybean, as observed for strains USDA110 and USDA122. The inability of USDA122 to nodulate *Rj2*-soybeans is mediated by the *Bradyrhizobium*-specific effector NopP2, with three amino acid residues (R60, R67, and H173) playing a role[9], Additionally, NopP2 of *B. diazoefficiens* Is-1 is incompatible with *Rj2*-soybean plants[15], whereas USDA110-NopP2 is more compatible with *Rj2*-soybeans. Therefore, rhizobia may use NopPs

and/or other T3Es as needed to promote symbiosis with their hosts. When comparing the amino acid sequences of NopP2 between USDA61 and USDA110 in relation to mutualistic symbiosis, and between USDA122 and ORS3257 in their negative interaction with the plant KPS1, the amino acid alignment revealed low similarity across all four strains (286 overlapping amino acid residues) (Fig. S4). The differences in amino acid sequences may cause USDA110-NopP2 to play a different role in mutualistic symbiosis with KPS1 than USDA61-NopP2 does. Perhaps, expressing USDA110-NopP2 directly in the *B. elkanii* USDA61 BEinnBnopP2 background could partially help demonstrate whether the protein itself has a positive regulatory effect on symbiosis, independent of its genomic background. Additionally, *Bradyrhizobium* species can generally nodulate *V. radiata* either efficiently or inefficiently, but the functions of NopPs from USDA61 remain unknown. Furthermore, *nopP1* and *nopP2* in the USDA61 genome were located within the symbiotic island near the *nif*-cluster, whereas *nopP1* was situated further from the symbiotic island and was located between transposases (Fig. S1). These findings implied that *nopP1* may have undergone horizontal gene transfer within the *B. elkanii* group. In addition, the features of NopP1 and NopP2 of USDA61, which have different numbers of amino acids (273 residues and 383 residues, respectively), revealed a putative secretion signal at the N-terminus (Fig. S5A). Research has shown that USDA61-NopP2 can be delivered into plant cells via the T3SS[16]. Furthermore, the three-dimensional structures of the NopP1 and NopP2 proteins were significantly different (Fig. S5B). These results suggest that the features and 3D structural models of NopPs indicate that USDA61-NopP1 and USDA61-NopP2 likely play different roles in mutualistic symbiosis with *V. radiata*. Therefore, it is worth studying the roles of USDA61-NopP in mutualistic interactions with KPS1 (Fig. 2).

We further functionally characterized the T3Es of USDA61, which control symbiotic interactions with the KPS1 cultivar. KPS1 established few nodules following inoculation with the wild-type strain (USDA61), whereas the nodulation efficiency drastically increased when the plants were inoculated with BEinnB. These findings indicate that USDA61-InnB is the key factor obstructing symbiosis with KPS1. However, the nodulation efficiency of BEinnB was significantly greater than that of the T3SS-deficient (BErhcJ) and InnB/NopP2 (BEinnBnopP2) double mutants, with nodule formation by BEinnBnopP2 not significantly different from that by BErhcJ. Therefore, NopP2 from USDA61 may be a crucial factor controlling KPS1 mutualism. In the case of the double mutation of InnB/Bel2-5 (BEinnB5208), the nodulation efficiency was similar to that of the single mutation of BEinnB, whereas the double mutation of InnB/nopP2 (BEinnBnopP2) drastically reduced the nodulation efficiency compared with that of BEinnB (Fig. S2). These results indicate that USDA61-Bel2-5 does not affect nodulation on KPS1, which is consistent with previous reports that Bel2-5 is not the main T3E controlling *V. mungo* symbiosis[10]. Therefore, we can conclude that USDA61-NopP2 is the key T3E that increases the efficiency of KPS1 symbiosis.

Indeed, the BEinnBnopP2 double mutation of USDA61 impaired both nodule organogenesis and young root nodule formation in KPS1 (Fig. 3A and C). Although the nodule morphology did not seem different between BEinnB and BEinnBnopP2, bacteroid cell death was more common in BEinnBnopP2 (Figs. 3B and 4). It seems that USDA61-NopP2 promotes nodulation and enhances bacteroid health. Similarly, a similar phenomenon was observed in the symbiotic interaction between *B. diazoefficiens* USDA110 and *V. radiata*, where a high number of nodules occasionally formed in inoculated KPS1 plants. In contrast, the USDA110-NopE1/E2-deficient strain nearly completely prevented nodulation[4]. These findings suggest that rhizobia have evolved different T3Es to inhabit the root nodules of *V. radiata*. Additionally, legumes may have developed multiple strategies to respond to different T3Es, thereby increasing the efficiency of their mutualistic relationships. In addition, in almost all Thai *V. radiata* cultivars, USDA61-NopP2 promoted symbiotic nodulation (Fig. 4 and Table S1), and nodule formation by BEinnBnopP2 was not significantly different from that by BErhcj. Perhaps USDA61-NopP2 is the key factor that promotes Thai *V. radiata-B. elkanii* USDA61 symbiosis. (Table S1). Our results suggest that USDA61-NopP2 might be directly recognized or indirectly recognized by an unknown specific *V. radiata* protein, consequently promoting nodulation. These results suggest that such symbiosis in *V. radiata* is likely induced through NFs in the absence of USDA61-NopP2, albeit weakly. Thus, USDA61-NopP2 may play complementary functions in modulating symbiosis and/or reducing *V. radiata* defense responses via unknown pathways to increase nodulation.

High-throughput sequencing and qRT-PCR are generally used to confirm the expression of transcripts (Fig. 5). Transcriptomes were analyzed in KPS1 to decipher how KPS1 responds to USDA61-NopP2. In this study, transcriptomic analysis was useful for identifying plant genes associated with BEinnB and BEinnBnopP2 inoculation (Fig. 5). The GO term analysis indicated that the number of downregulated genes was greater than the number of upregulated genes related to biological processes such as nodulation, gibberellin biosynthetic processes, cellular components, and the peribacteriod membrane after BinnBnopP2 inoculation. It is related to the network of metabolic pathways, such as their growth, development, and nodule formation. It seems that USDA61-NopP2 facilitate KPS1 symbiosis. The expression of some intermediates of GA signaling-related genes (GA20ox), fotillin-like gene 4 (FLOT4), ENOD55, nodulin 26 and CASP-24 was suppressed by BEinnBnopP2 compared with BEinnB. Because nodule organogenesis is systemically controlled by legume plants, several phytohormones are regulated in response to rhizobia NFs and USDA61-NopP2. In addition, the biosynthesis of gibberellic acid (GA) in legumes requires enzymes such as GA20 oxidase (GA20ox), which is a rate-limiting factor that involves intermediate steps in GA production[17]. Our results revealed that GA20ox is more highly expressed in BEinnB roots than in BEinnBnopP2 roots at 4 dpi. This finding is consistent with previous reports in *Sesbania rostrata* and *V. radiata*, where GA20ox is primarily upregulated in plant tissues involved in infection and nodule primordia formation[4,18], indicating that USDA61-NopP2 is a factor related to legume GA production. Moreover, FLOT4 was also significantly expressed in BEinnB compared with BEinnBnopP2 inoculation, similar to FLOT4 of *S. meliloti*, which is localized to the infection thread membrane of *Medicago truncatula*, and it plays an important role in symbiotic bacterial infection[19]. CASP-24, nodulin 26, and ENOD55/ENOD75 are also factors expressed very early in the development of the root nodules of legumes[20–22]. In KPS1,

USDA61-NopP2 appears to play a role in enhancing the expression of genes related to infection and nodule organogenesis, which are important for the nodulation process. Additionally, this is a novel finding regarding the mechanism of USDA61-NopP2 and its interaction with plant biomolecules, as USDA61-NopP2 can interact with pathogenesis-related protein 10 (PR10) (Fig. 7). The PR10 protein is part of the plant's defense against biotic stresses. PR10 proteins can collaborate with other factors to participate in pathogen resistance[23,24]. Research has shown that the expression of the *PR10* gene increases in the roots and nodules of *M. truncatula* when it is invaded by microorganisms[25]. Therefore, USDA61-NopP2 may bind to KPS1-PR10, resulting in the inactivation of the role of PR10. This, in turn, may enhance the mutualistic relationship between BEinnB and KPS1 compared with BEinnBnopP2. However, PR10 performs various functions, including binding to hormone molecules, interacting with secondary metabolites, and defending against biotic and abiotic stressors[23]. The role of PR10 in the development of root nodules in KPS1 is not clearly understood and may be a subject for future research. We propose a model modulated by USDA61-NopP2 in Fig. 8. The USDA61-NopP2 effector is required to optimize nodulation efficiency by interacting with the plant PR10 protein, which is deleterious to rhizobial infection. Therefore, USDA61-NopP2 can trigger nodulation by modulating the expression of genes related to infection and nodule organogenesis in KPS1.

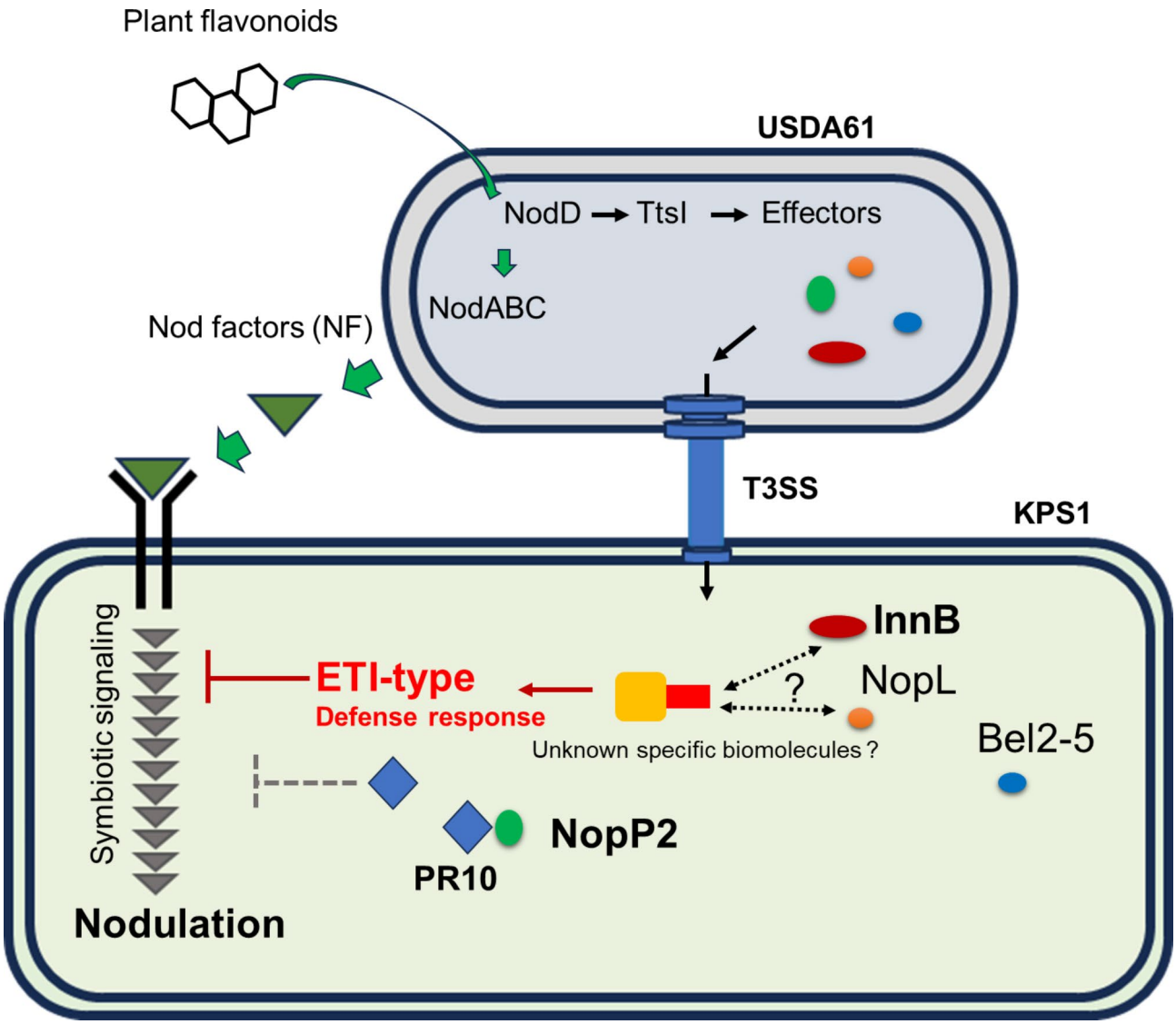

Fig. 8. Putative models of host genotype-specific symbiotic interactions between *B. elkanii* USDA61 and *V. radiata* KPS1 may be controlled mainly by the two type III effectors InnB and NopP2. Hypothetically, InnB might be recognized by unknown biomolecule(s) or a specific resistance (R) protein in legumes, consequently activating an R protein-mediated ETI-type defense. In contrast, NopP2 is a nodulation determinant that enables the nodulation of *V. radiata* KPS1 by interacting with the pathogenesis-related 10 (PR10) protein, thereby reducing the defense response (ETI-type) to inhibit nodulation. The dotted line indicates unclear symbiotic mechanisms.

Materials and methods

Microbiological and molecular techniques

Bradyrhizobium elkanii USDA61 and its mutant strains were grown at 28 °C in arabinose-gluconate (AG) medium[26], and *Escherichia coli* was grown on LB medium at 37 °C[27]. The bacteria and plasmids used are summarized in Table S2, and the antibiotic concentrations that were added to the media as follows (μg/ml): ampicillin, 100; kanamycin, 200; and polymyxin, 50. For USDA61-*nopP2* complementation, the USDA61-*nopP2* gene was amplified (including the *tts* box promoter region) by PCR were cloned and inserted into the plasmids pMG103 sm/sp and km-gfp. The primers used are listed in Table S3. The electrocompetent cells of BEinnBnopP2 were prepared by growing bacterial cells in AG medium until the OD600 of the cells reached 0.4–0.6. The bacterial cells were subsequently harvested by centrifugation at 4,000 rpm for 15 min, carefully washed twice with cold sterilized water and finally resuspended in 10% cold glycerol (stored at − 80 °C before use). The plasmid transformation was carried out using electroporation with capacitor settings of 25 μF, 100 Ω, and a voltage of 1.75 kv/cm for 0.2 cm cuvettes, and the complement strain was selected on AG agar plates with appropriate antibiotics.

Plant materials and nodulation assays

The 12 genotypes of *Vigna radiata* that were tested are provided by Professor Piyada Alisha Tantasawat, all *Vigna radiata* genotypes were Thai published varieties that are normally cultivated by Thai farmers (KPS1, KPS2, SUT1, SUT2, SUT3, SUT4, SUT5, M4-2, M5-1, CN36, CN72 and CN84-1)[4] (Table S4). This study complies with local and national regulations in Thailand. The *V. radiata* seeds used were sterilized and subsequently germinated as described previously[4]. Five days after transplantation, the seedlings were inoculated with USDA61 and its derivative mutants (1 ml of 10^7 cells ml^{-1} per seedling). The plants were watered with BNM solution[28] and grown under the following controlled environmental conditions: 28 ± 2 °C and 70% relative humidity under a 16 h light/8 h dark photoperiod and a light intensity of 300 μE/m^2/s. The *V. radiata* symbiotic phenotypes were analyzed at 11, 15, and 30 dpi by evaluating the nodule image, nodule number, nodule fresh weight, whole-plant dry weight, and nodule primordia formation.

Cytological analysis of nodules

A nodule image was examined using a Leica Microsystems EZ4 Stereo Microscope (Leica, Nanterre, France). Fresh nodules were embedded in 5% agar and sectioned into 40–50 μm thick slices with a VT1000S vibratome (Leica, Nanterre, France). The nodule sections were immersed in a live/dead staining solution (5 μM SYTO 9 and 30 μM propidium iodide in 50 mM Tris buffer, pH 7.0) for 15 min. To stain the plant cell wall, the nodule sections were additionally incubated for 20 min with calcofluor white M2R (0.01% (wt/vol) calcofluor white M2R in 10 mM phosphate saline buffer). The stained nodules were then observed under an inverted confocal microscope using a Nikon A1Rsi (Nikon, USA). Lasers were used to detect Calcofluor, SYTO-9, and propidium iodide (PI) as follows: Calcofluor white was excited at 405 nm and detected using a 460–500 nm emission filter. For SYTO-9 and PI, excitation wavelengths of 488 nm and 555 nm, respectively, were used to collect emission signals at 490–522 nm and 555–700 nm.

V. radiata KPS1 mRNA transcriptome

For RNA-seq, KPS1 seeds were surface sterilized and germinated at 25 °C for one day. They were then transplanted into Leonard's jars and watered with BMN solution. After five days of growth, the KPS1 seedlings were inoculated with 1 ml of bacterial cell culture containing 10^7 cells ml^{-1}. At 4 dpi, the KPS1 roots were washed and immediately transferred to liquid nitrogen. The frozen roots were then ground into a fine powder. Total RNA was subsequently extracted from 100 mg of root powder using the RNeasy Plant Mini Kit (Qiagen) with DNase I treatment, following the manufacturer's instructions. Reverse transcription of 4 μg of total RNA was performed according to the manufacturer's protocol for the TruSeq Stranded mRNA LT Sample Prep Kit (Illumina). Each library was sequenced using the Illumina platform, and the sequences were analyzed using a bioinformatics approach via GENEWIZ in Suzhou, China. Differentially expressed genes (DEGs) were selected for further analysis on the basis of a Padj value of less than 0.05 and a fold change greater than 1.5. Data is provided within supplementary information files.

qRT–PCR of DEGs

The selected DEGs of KPS1 were further analyzed via qRT-PCR using the same protocol described above. The primers used for qRT-PCR are listed in Table S4. The PCR amplification program included an initial denaturation step at 95 °C for 2 min, followed by 40 cycles at 95 °C for 30 s, 60 °C for 30 s, and 72 °C for 30 s, with a final extension step at 72 °C for 10 min. Relative gene expression was analyzed using the comparative Ct (−ΔΔCT) method[29], and the transcript levels of selected *V. radiata* DEGs were normalized to the expression of the housekeeping gene *β-actin*[30–35]. The data for each sample were calculated from three biological replicates.

KPS1 root protein extraction

KPS1 was used for root protein extraction. Five days after transplantation, the seedlings were inoculated with USDA61 or its derivative mutant BEinnB (1 ml of 10^7 cells ml^{-1} per seedling). The KPS1 roots were collected at 1 dpi and 2 dpi and then immediately frozen in liquid nitrogen. Three grams of roots were ground into a fine powder under liquid nitrogen and mixed with 10 ml of extraction buffer (0.5 M Tris-HCl, 10% sucrose, 3 mM PMSF, 10 mM ascorbic acid, 0.2% Triton X-100 and 1% β-mercaptoethanol; pH 8.0). The root extraction buffer was centrifuged at 12,000 × g at 4 °C for 20 min, and the organic phase was transferred into a new tube. Then, 7.5 ml of Tris-EDTA-saturated phenol and 1 ml of 1 M dithiothreitol (DTT) were added. The solution was mixed thoroughly and centrifuged again at 12,000 × g at 4 °C for 20 min. The phenol phase was transferred into a new

tube containing 20 ml of methanol, 300 µl of 8 M ammonium acetate, and 400 µl of 1 M DTT. The solution was mixed well and stored at -20 °C overnight. The mixture was subsequently centrifuged at 4 °C and 10,000 × g for 10 min, followed by resuspension with 1 ml of 70% ethanol for washing. After centrifugation, the ethanol was removed, and the pellet was air dried. The root proteins were resuspended to saturation in Tris-HCl (20 mM, pH 7.4) and quantified according to the Bradford method[36].

Recombinant protein production of NopP2, adenosyl homocysteinase and pathogen-related protein 10

To construct expression vectors for recombinant protein production, the NopP2 and adenosyl homocysteinase genes were cloned and inserted into the pGEX4T-3 vector, and the coding sequence for pathogen-related protein 10 was cloned and inserted into the pET22b vector. The recombinant plasmid was subsequently transformed into *E. coli* BL21 for expression. *E. coli* BL21 harboring the recombinant plasmid was grown at 37 °C in 5 ml of LB medium supplemented with 100 µg/ml ampicillin with shaking at 200 rpm and 37 °C overnight. 1% v/v of each overnight culture was inoculated into LB medium supplemented with 100 µg/ml ampicillin. The culture was subsequently incubated with shaking at 37 °C until the OD 600 reached 0.4–0.6. The induction was performed by adding 1 M isopropyl-βd-thiogalactopyranoside (IPTG) to achieve a final concentration of 1 mM. After the cells were grown for 4 h at 30 °C with shaking, they were collected by centrifugation at 16 °C and 8,000 rpm for 15 min and resuspended in buffer (20 mM Tris-HCl, 150 mM NaCl, and 20 mM imidazole; pH 7.4). Sonication was then performed before the purification of the recombinant protein. The GST/hexahistidine tag was used for detection and purification. The protein concentration was quantified by the Bradford method, and the purity of the purified protein was determined via SDS–PAGE and Western blotting with mouse anti-GST (Abbkine, USA) or mouse anti-HSI (Abbkine, USA) and goat anti-mouse conjugated HRP.

Pull-down assay

To identify novel interacting partners the predicted protein–protein interaction, a pull-down assay was performed to investigate protein–protein interactions between NopP2 and the root protein. The purified rNopP2-GST fusion protein was attached to glutathione beads. The extracted root protein was added and incubated at 4 °C overnight. The protein mixture was then washed twice with phosphate-buffered saline (PBS). Elution of the GST-tagged proteins was performed by adding 50 mM reduced glutathione in 100 mM Tris, pH 7.4. The total amount of eluted protein was subsequently analyzed using polyacrylamide gel electrophoresis. The distinct bands of the rNopP2-GST/root, compared with those of root protein and rNopP2-GST, were identified and excised for SDS-MS/MS analysis. The LC-MS/MS system consists of a liquid chromatograph (Dionex Ultimate 3000, RSLCnano System, Thermo Fisher Scientific, Waltham, MA, USA) in combination with a captivespray ionization/mass spectrometer (Model Q-ToF Compact, Bruker, Germany) at the Proteomics Services, Faculty of Medical Technology, Mahidol University (Salaya Campus, Mahidol University, Nakhon Pathom, Thailand). Mass spectral data from 300 to 1500 m/z were collected in positive ionization mode. In order to confirm the interaction of candidate root proteins (rAD and rPR10), rNopP2-GST fusion protein or recombinant root proteins were attached to glutathione beads or Ni-NTA agarose bead. The protein-protein interaction was again carried out by pull-down assay and detected by western blot analysis as describe below.

Western blot analysis

The recombinant proteins were blotted onto nitrocellulose membranes (Bio-Rad, USA) from the SDS polyacrylamide gel using a membrane transfer machine. The membrane was blocked with PBS containing skim milk (5% MPBS) for 1 h, followed by washing with PBS twice. After that, mouse anti-GST (Abbkine, USA) and/or mouse anti-HIS (Abbkine, USA) were used to detect the GST tag/HIS tag. The membrane was incubated with primary antibody at a dilution of 1:5000 in PBS for 1 h, followed by 3 washes with PBS supplemented with 0.05% Tween 20 detergent (PBST) and 2 washes with PBS. After that, goat anti-mouse conjugated HRP (Abbkine, USA) diluted 1:5000 in PBS was added, and the membrane was incubated for 1 h before development. The enhanced chemiluminescence (ECL) substrate (Cytiva, USA) was used according to the manufacturer's protocol for developing the signals on the membrane.

ELISA

The binding affinity of NopP2 for PR10 was determined by ELISA according to the protocol of Eble[37] with some modifications. An Immuno96 microwell plate (Nunc, Denmark) was used to immobilize 5 µg of rPR10-HIS in 100 µl of 100 mM $NaHCO_3$, pH 9.0, at 4 °C overnight. The wells were rinsed 3 times with PBS to remove any non-specific binding, followed by stabilization with 100 µl of stabilizer (5% sucrose, 0.3% BSA, and 50 mM $NaHCO_3$) for 45 min. The wells were rinsed with PBS twice and blocked with 0.5% (w/v) BSA at room temperature for 1 h. After that, the wells were rinsed 4 times with PBST and 2 times with PBS. Then, 0–5 µM rNopP2-GST or rGST was added to the wells and incubated at room temperature for 1 h. The wells were washed 4 times with PBST, followed by 2 washes with PBS before the addition of the antibody against the GST tag mouse anti-GST (1:5000). The wells were washed 4 times with PBST, followed by 2 washes with PBS. After the plates were incubated at room temperature for 1 h, a 1:5000 dilution of goat anti-mouse conjugated HRP in 100 µl of PBS was added to each well, and the mixture was incubated at room temperature for 1 h. The wells were washed 4 times with PBST followed by 2 washes with PBS. The color of the reaction was developed by adding 200 µl of ABTS substrate (Wako, Japan), and the plates were incubated at room temperature for 5 min before the absorbance was measured at 405 nm with an ELISA plate reader.

Phylogenetic construction and statistical analysis

For phylogenetic and evolutionary analyses, NopP homologs were queried via BLASTx against genomic databases of rhizobial species. A phylogenetic tree was constructed using the Maximum Likelihood method from the MEGA 11.0 package. The analysis used the Jones-Taylor-Thornton (JTT) and Gamma Distributed (G) models, with 1,000 bootstrap replications. For statistical analyses, one-way analysis of variance (ANOVA) followed by post hoc tests (Tukey's tests at $P \leq 0.05$) was performed using Minitab version 16.0 for multiple test sample comparisons. Two-tailed Student's t tests were also performed for pairwise comparisons when needed. P values < 0.05 were considered statistically significant. The sample size and replications are detailed in the figure and table legends.

Data availability

All data generated or analysed during this study are included in this published article (and its Supplementary Information files). The RNA sequences generated in this study were deposited in NCBI under accession numbers PRJNA1167634.

Received: 17 July 2024; Accepted: 3 October 2024
Published online: 19 October 2024

References

1. Oldroyd, G. E. D. Speak, friend, and enter: Signalling systems that promote beneficial symbiotic associations in plants. *Nat. Rev. Microbiol.* **11**, 252–263 (2013).
2. Krause, A., Doerfel, A. & Göttfert, M. Mutational and transcriptional analysis of the type III secretion system of *Bradyrhizobium Japonicum*. *Mol. Plant-Microbe Interact.* **15**, 1228–1235 (2002).
3. Wassem, R. et al. TtsI regulates symbiotic genes in *Rhizobium* species NGR234 by binding to tts boxes. *Mol. Microbiol.* **68**, 736–748 (2008).
4. Piromyou, P. et al. The *Bradyrhizobium diazoefficiens* type III effector NopE modulates the regulation of plant hormones towards nodulation in *Vigna radiata*. *Sci. Rep.* **11**, 1–12 (2021).
5. Dai, W. J., Zeng, Y., Xie, Z. P. & Staehelin, C. Symbiosis-promoting and deleterious effects of NopT, a novel type 3 effector of *Rhizobium* sp. strain NGR234. *J. Bacteriol.* **190**, 5101–5110 (2008).
6. Skorpil, P. et al. NopP, a phosphorylated effector of *Rhizobium* sp. strain NGR234, is a major determinant of nodulation of the tropical legumes *Flemingia congesta* and *Tephrosia vogelii*. *Mol. Microbiol.* **57**, 1304–1317 (2005).
7. Jiménez-Guerrero, I. et al. The *Sinorhizobium* (*Ensifer*) *fredii* HH103 nodulation outer protein NopI is a determinant for efficient nodulation of soybean and cowpea plants. *Appl. Environ. Microbiol.* **83**, 1–13 (2017).
8. Songwattana, P. et al. Identification of type III effectors modulating the symbiotic properties of *Bradyrhizobium vignae* strain ORS3257 with various *Vigna* species. *Sci. Rep.* **11**, 4874. https://doi.org/10.1038/s41598-021-84205-w (2021).
9. Sugawara, M. et al. Variation in bradyrhizobial NopP effector determines symbiotic incompatibility with Rj2-soybeans via effector-triggered immunity. *Nat. Commun.* **9**, 3139. https://doi.org/10.1038/s41467-018-05663-x (2018).
10. Nguyen, H. P., Ratu, S. T. N., Yasuda, M., Teaumroong, N. & Okazaki, S. Identification of *Bradyrhizobium elkanii* USDA61 type III effectors determining symbiosis with *Vigna mungo*. *Genes* **11**, 474. https://doi.org/10.3390/genes11050474 (2020).
11. Miwa, H. & Okazaki, S. How effectors promote beneficial interactions. *Curr. Opin. Plant. Biol.* **38**, 148–154 (2017).
12. Staehelin, C. & Krishnan, H. B. Nodulation outer proteins: Double-edged swords of symbiotic Rhizobia. *Biochem. J.* **470**, 263–274 (2015).
13. Nguyen, H. P., Miwa, H., Kaneko, T., Sato, S. & Okazaki, S. Identification of *Bradyrhizobium elkanii* genes involved in incompatibility with *Vigna radiate*. *Genes* **8**, 374. https://doi.org/10.3390/genes8120374 (2017).
14. Nguyen, H. P., Ratu, S. T. N., Yasuda, M., Göttfert, M. & Okazaki, S. InnB, a novel type III effector of *Bradyrhizobium elkanii* USDA61, controls symbiosis with *Vigna* species. *Front. Microbiol.* **9**, 3155. https://doi.org/10.3389/fmicb.2018.03155 (2018).
15. Ishizuka, J., Yokoyama, A. & Suemasu, Y. Relationship between serotypes of *Bradyrhizobium japonicum* and their compatibility with Rj-cultivars for nodulation. *Soil. Sci. Plant. Nutr.* **37**, 23–30 (1991).
16. Okazaki, S., Zehner, S., Hempel, J., Lang, K. & Göttfert, M. Genetic organization and functional analysis of the type III secretion system of *Bradyrhizobium elkanii*. *FEMS Microbiol. Lett.* **295**, 88–95 (2009).
17. Hedden, P. The current status of research on gibberellin biosynthesis. *Plant. Cell. Physiol.* **61**, 1832–1849 (2020).
18. Lievens, S. et al. Gibberellins are involved in nodulation of *Sesbania rostrata*. *Plant. Physiol.* **139**, 1366–1379 (2005).
19. Haney, C. H. & Long, S. R. Plant flotillins are required for infection by nitrogen-fixing bacteria. *Proc. Natl. Acad. Sci. U.S.A.* **107**, 478–483 (2010).
20. Okazaki, S., Kaneko, T., Sato, S. & Saeki, K. Hijacking of leguminous nodulation signaling by the rhizobial type III secretion system. *Proc. Natl. Acad. Sci. U S A.* **110**, 17131–17136 (2013).
21. Rivers, R. L. et al. Functional Analysis of Nodulin 26, an aquaporin in soybean root nodule symbiosomes. *J. Biol. Chem.* **272**, 16256–16261 (1997).
22. Franssen, H. J. et al. Characterization of cDNA for nodulin-75 of soybean: A gene product involved in early stages of root nodule development. *Proc. Natl. Acad. Sci. U S A.* **84**, 4495–4499 (1987).
23. Lopes, N. et al. Pathogenesis-related protein 10 in resistance to biotic stress: progress in elucidating functions, regulation and modes of action. *Front. Plant. Sci.* **14**, 1193873. https://doi.org/10.3389/fpls.2023.1193873 (2023).
24. Sinha, R. K., Verma, S. S. & Rastogi, A. Role of pathogen-related protein 10 (PR 10) under abiotic and biotic stresses in plants. *Phyton* **89**, 167–182 (2020).
25. Gamas, P., De Billy, F. & Truchet, G. Symbiosis-specific expression of two *Medicago* Nodulin genes, MtN1 and MtN13, encoding homologous to Plant Defense proteins. *Mol. Plant-Microbe Interact.* **11**, 393–403 (1998).
26. Sadowsky, M. J., Tully, R. E., Cregan, P. B. & Keyser, H. H. Genetic diversity in *Bradyrhizobium japonicum* Serogroup 123 and its relation to genotype-specific nodulation of soybean. *Appl. Environ. Microbiol.* **53**, 2624–2630 (1987).
27. Wood, E. Molecular cloning A: Laboratory manual. *Biochem. Educ.* **11**, 82 (1983).
28. Ehrhardt, D. W., Atkinson, M., Long, S. R. & E. & Depolarization of alfalfa root hair membrane potential by *Rhizobium meliloti* nod factors. *Science* **256**, 998–1000 (1992).
29. Livak, K. J. & Schmittgen, T. D. Analysis of relative gene expression data using real-time quantitative PCR and the 2-ΔΔCT method. *Methods* **25**, 402–408 (2001).
30. Narancio, R., John, U., Mason, J. & Spangenberg, G. Selection of optimal reference genes for quantitative RT-PCR transcript abundance analysis in white clover (*Trifolium repens* L). *Funct. Plant. Biol.* **45**, 737–744 (2018).
31. Chi, C. et al. Selection and validation of reference genes for gene expression analysis in *Vigna angularis* using quantitative real-time RT-PCR. *PLoS One* **11**, e0168479. https://doi.org/10.1371/journal.pone.0168479 (2016).

32. Ke, X. W. et al. Reference genes for quantitative real-time PCR analysis of gene expression in mung bean under abiotic stress and *Cercospora canescens* infection. *Legume Res.* **44**, 646–651 (2021).
33. Kundu, A., Patel, A. & Pal, A. Defining reference genes for qPCR normalization to study biotic and abiotic stress responses in *Vigna mungo*. *Plant. Cell. Rep.* **32**, 1647–1658 (2013).
34. Dasgupta, U. et al. Comparative RNA-Seq analysis unfolds a complex regulatory network imparting yellow mosaic disease resistance in mungbean [*Vigna radiata* (L.) R. Wilczek]. *PLoS One* **16**, e0244593. https://doi.org/10.1371/journal.pone.0244593 (2021).
35. Bjarnadottir, H. & Jonsson, J. J. A rapid real-time qRT-PCR assay for ovine β-actin mRNA. *J. Biotechnol.* **117**, 173–182 (2005).
36. Bradford, M. M. A rapid and sensitive method for the quantitation of microgram quantities of protein utilizing the principle of protein-dye binding. *Anal. Biochem.* **72**, 248–254 (1976).
37. Eble, J. A. Titration elisa as a method to determine the dissociation constant of receptor ligand interaction. *J. Vis. Exp.* e57334 (2018). https://doi.org/10.3791/57334 (2018).

Acknowledgements

This work was supported by (i) Suranaree University of Technology (SUT), (ii) Thailand Science Research and Innovation (TSRI), and (iii) National Science, Research, and Innovation Fund (NSRF) (grant number 195582), (iv) NSRF via the Program Management Unit for Human Resources & Institutional Development, Research, and Innovation (grant number B13F660055), (v) JSPS-NRCT by National Research Council of Thailand (grant number N11A670769). (vi) The Office of the Permanent Secretary of the Ministry of Higher Education, Science, Research and Innovation.

Author contributions

ContributionsP.P., H.P.N., P.S., P.T., N.B., K.T., T.G., P.N., J.W., S.S. and N.T. designed the experiments. P.P., H.P.N., N.P., S.O., P.B. and N.T. performed the experiments and analysed the data. P.P., S.O., and N.T. wrote the paper.

Declarations

Competing interests

The authors declare no competing interests.

Additional information

Supplementary Information The online version contains supplementary material available at https://doi.org/10.1038/s41598-024-75294-4.

Correspondence and requests for materials should be addressed to P.B., S.O. or N.T.